Springer

Journal of Mechanical Science and Technology 23 (2009) 2244~2252

Journal of Mechanical Science and Technology

www.springerlink.com/content/1738-494x
DOI 10.1007/s12206-009-0517-y

Modeling high-speed impacts and explosions with ExLO code †

Wan-Jin Chung[1] and Minhyung Lee[2,*]

[1]*Department of Die & Mould Engineering, Seoul National University of Technology, Seoul, 139-743 Korea*
[2]*Department of Mechanical Engineering, Sejong University, 98 Kunja-Dong, Kwang-Jin Gu, Seoul, 143-747 Korea*

(Manuscript Received February 22, 2008; Revised March 10, 2009; Accepted April 22, 2009)

Abstract

Korea has recently developed a total shock physics code, ExLO, based on the three-dimensional finite element method in order to calculate highly transient events involving large deformations. One special feature of the code is that the Lagrangian, ALE and Eulerian schemes are integrated into a single framework. The details of the numerical schemes are described in a previous paper [1]. In this paper, the modeling capability of ExLO has been described for two extreme loading events: high-speed impacts and explosions. Results of three-dimensional calculations for penetration of long rods and segments (L/D < 1) into thick target show a good agreement with experimental results and other finite difference solutions. Next, we include the free field air blast modeling by two approaches, one-dimensional spherical coordinates and three-dimensional rectangular coordinates. The predictions are compared with an analytic solution of air blast. For large scale simulations required for complex design problems, some advances in the field of parallelization and adaptive meshing are demanded.

Keywords: ExLO; High-speed impact; Explosion

1. Introduction

Studies of highly transient events rely on heavy use of computer simulations. Simulations are used in the detailed analysis of experiments. They can also be applied to the areas that are expensive or too impractical to explore experimentally. Hence, significant efforts have been devoted to develop the models and computer codes [2]. Highly dynamic events can arise in industrial applications such as high-speed machining [3] and shock processing of powders, and in military applications such as high speed projectile-target impact, shaped-charge jets, air blast and underwater explosions [4]. The fundamental features of the problems listed above are categorized by the nonlinear wave propagation and huge strain rate associated with high-speed multi-material interactions.

In 2004, an effort was launched in Korea to develop a state-of-the-art code that combined the Lagrangian, ALE and Eulerian schemes. This code is called ExLO. To validate the schemes a benchmark problem such as Taylor impact of a copper rod was already well compared with the existing experimental data [1]. In this paper, modeling with ExLO is presented for computing highly transient dynamic problems of two extreme areas such as munition-target impacts and explosions. Here the Eulerian scheme has been applied to these applications.

2. Summary of an ExLO code

ExLO has been developed as a three-dimensional explicit dynamic program based on the finite element method and written in C++. By employing a splitting algorithm to the governing equations, the Lagrangian,

† This paper was recommended for publication in revised form by Associate Editor Heoung Jae Chun

*Corresponding author. Tel.: +82 2 3408 3282, Fax.: +82 2 3408 4333
E-mail address: mlee@sejong.ac.kr

ALE and Eulerian schemes have been combined into a single framework. This enables ExLO to be applicable for a wide variety of design problems including fluid-structure interactions (FSIs), or otherwise, for FSIs two separate codes need to be interfaced.

Currently, an eight node brick element is employed with one point integration scheme to prevent locking. The material models are elastic-plastic behavior, Johnson-Cook fracture model and null model. Several equations of state (EOS) are available such as the Jones-Wilkins-Lee (JWL) for high explosive reactive products, the ideal gas, and the Mie- Gruneisen type. Piecewise-constant [5] and piecewise-linear [6] material interface construction schemes provide the basis for material interfaces between multi materials in a mixed cell. During the interface tracking, the critical volume fraction F_c is typically set to 1.0^{-4}. For cell-centered properties such as mass and internal energy, an upwind scheme, which is first-order, is adopted. To reduce dispersion, a second-order scheme is also included in the code [7, 8]. Finally, vertex-centered advection is based on the SALE algorithm [9] and some modifications are incorporated. Two mixture theories studied are the equal strain rate model and linearized pressure equilibrium model. More details are included in a separate paper in this volume [1]. To demonstrate the capabilities of ExLO, we simulated a variety of problems of interest in the high-speed impacts and explosions. These are discussed below.

3. Modeling of high-speed impacts

In this section, validation of our schemes is tested for high-speed impact/penetration problems between two different deformable objects. Three-dimensional calculations were conducted in rectangular coordinates, and the numerical results are compared with existing experimental data or empirical correlations.

3.1 Three-dimensional penetration of WHA rod into thick steel target

First, a series of simulations were conducted for L/D =5 tungsten rod penetrating thick 4030 steel target at velocities ranging from 1000, 1500 and 2000 *m/s*. Here L is the rod length and D is the rod diameter. Table 1 shows the material properties used for WHA and steel. A von Mises with a kinematic hardening parameter β is used. Due to two symmetry planes, as shown in Fig. 1, the computational domain is one-quarter of a block. The thickness of the target along the penetration direction is three times the rod length. To ensure reasonable computational effort, the width

Table 1. Material properties for von Mises model with kinematic hardening.

	ρ_o (kg/m^3)	E (GPa)	poison ratio	Y (GPa)	Kinematic hardening
Tungsten alloy	17100	190.8	0.3	1.80	1.0
steel	7830	416.0	0.3	0.79	1.0

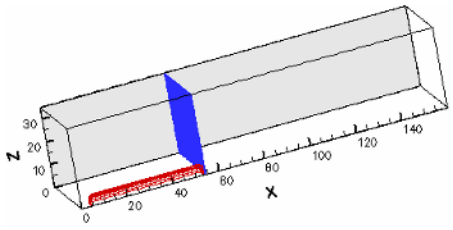

Fig. 1. Three-dimensional calculation of a rod impact into a thick target at 1500 m/s.

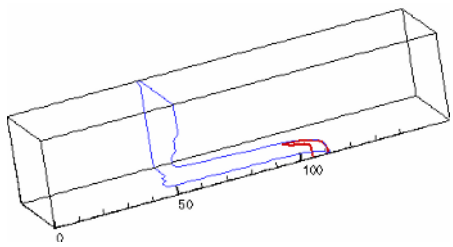

(a)

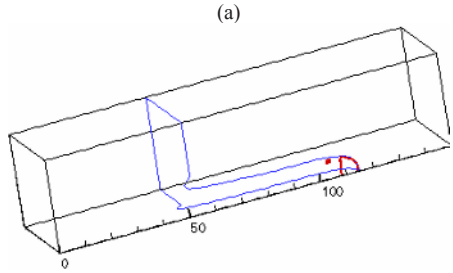

(b)

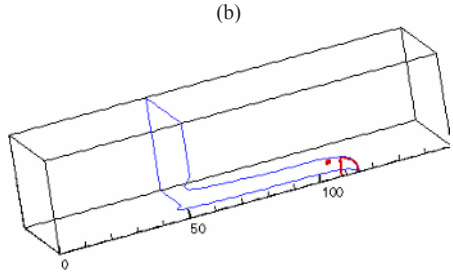

(c)

Fig. 2. Final shapes of a tungsten rod penetrating a thick target using (a) 80×35×35 mesh, (b) 120×35×35 mesh, and (c) 150×35×35 mesh.

of target block is limited to eight times the rod radius.

A grid independence study is first carried out at the impact velocity of 1500 *m/s*. Three meshes tested are 80×35×35 (total cells 98,000), 120×35×35, and 150×35×35 (more cells along the penetration direction). The final shapes (at 80 μs) of the deformed bodies are shown in Figs. 2(a), (b), (c) using three-dimensional contour. It can be seen that the penetration depth is not changed at the finest mesh system. For now, the 120×35×35 mesh is used for other cases. The typical penetration processes are illustrated in Fig. 3 at three time steps. The main features of the long rod penetration into a thick target are well captured. To evaluate the accuracy of the numerical results, the final penetration depth is calculated for several impact velocities. The predictions are compared with an empirical correlation [10],

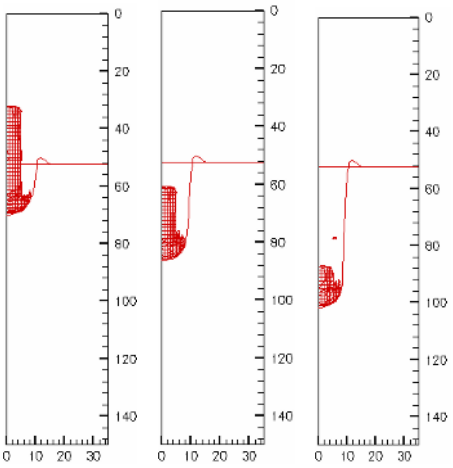

(a) 20 μs (b) 40 μs (c) 60 μs

Fig. 3. Shapes of a tungsten rod penetrating a thick steel target, impact velocity 1500 m/s.

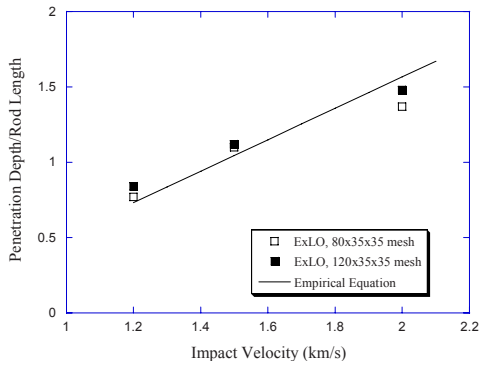

Fig. 4. Penetration depth (*P*/*L*) comparisons for *L*/*D* = 5 rod.

$$\frac{P}{L} = -0.209 + 1.044\left(\frac{U}{U_o}\right) - 0.194\ln\left(\frac{L}{D}\right), \quad \text{for } 1.2 < U/U_o < 1.8 \text{ and } 5 < L/D < 30, \tag{1}$$

where $U_o = 1.0\ km/s$. The results of *P*/*L* are summarized in Fig. 4, where *P* is the penetration depth. The difference between two different meshes is within 8 %. Most of all, a good agreement is obtained within a reasonable range for all three impact velocities. This reveals that the truncated domain size and the mesh size seem to be fairly good in terms of the computational economy for the three-dimensional calculation.

3.2 A segment impact into thick target

Recently, some studies have been conducted on different types of impacting body to enhance the penetration capability while the total mass remains constant. One type is the segmented-rod consisting of multiple, small aspect ratio segments (1/8 < *L*/*D* < 1). As the aspect ratio of a body decreases and the body becomes more disk like, the penetration mode changes. To understand the penetration mechanics, numerical [11], experimental [12-14] and analytical studies [15] were carried out.

The ultimate question is how much the penetration depth can be increased when a long body is broken into segments. Early studies which analyzed the penetration mechanics of a single segment indicate that the penetration performance (*P*/*L*) increases with decreasing *L*/*D*. However, as far as a train of segment is concerned, more design parameters such as the aspect ratio, impact velocity, and spacing between each segment need to be investigated in order to provide some answers. The previous results of numerical calculation showed that for successive segments some degradation in penetration performance is more pronounced for segments of smaller aspect ratios [16]. Hence, more issues still have to be answered for a specific design.

One difficulty associated with the experimental study is that it is hard to make a perfectly aligned train of segments. Hence, numerical simulations in which all parameters and geometry conditions are well predetermined can provide a good methodology especially for this problem. In this section a series of three-dimensional calculations are conducted for tungsten segments of *L*/*D*s ranging from 1 to 1/4 penetrating a thick 4030 steel target. The impact ve-

locities considered are 1.5 km/s and 2.0 km/s. The same material properties with the previous section were also used here. Eulerian modeling is suitable for such deep penetration and high-speed impact problems. The three-dimensional domain in this study is not a quarter block but a half block, just for checkup. The result is the same. The domain is modeled by either 100×80×40 (total cells 320,000) or 80×80×40 (total cells 256,000). In general, zoning is 10 cells across the length of the disk. It usually takes 3 hours until the segment completely stops on a personal computer with 2G memory.

The penetration processes of a L/D = 1/4 segment into a thick target at an impact velocity of 1.5 km/s is illustrated in Fig. 5. The segment is more like a disk and plain symmetry waves are produced, which is different from the case of long rod impact. The main features of a disk penetration into a thick target are well simulated. Fig. 6 shows the penetration processes of L/D = 1 segment into thick target at the same impact velocity. The final crater profiles and residual segments can also be compared with Figs 5 and 6 for different aspect ratio segment.

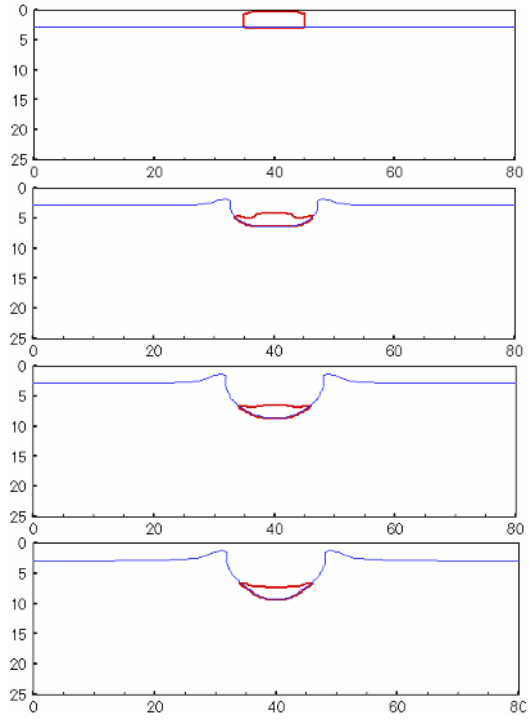

Fig. 5. Penetration processes of disk-shaped segment (L/D = 1/4) into thick target using 80×80×40 Eulerian mesh (256,000 cells), t = 0, 5, 10 and 20 μs.

Since the kinetic energy of the segment is proportional to the length for equal diameter and constant impact velocity, it is certain that the penetration depth

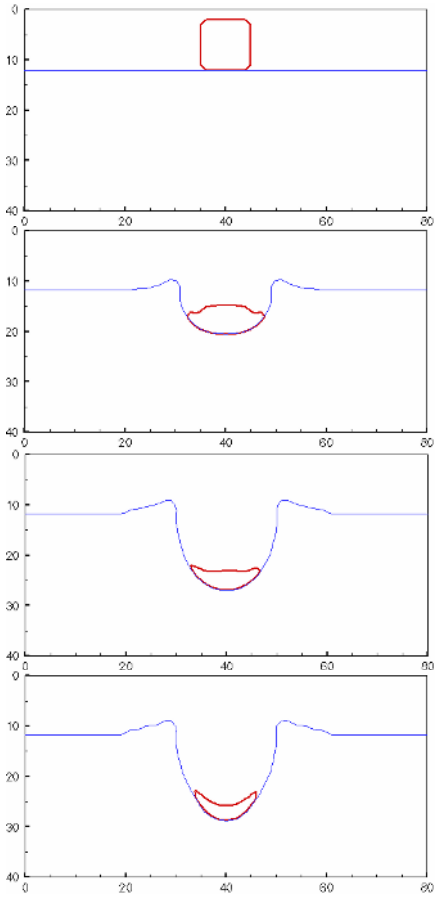

Fig. 6. Penetration processes of disk-shaped segment (L/D = 1) into thick target using 10×80×40 Eulerian mesh (320,000 cells), t = 0, 10, 20 and 30 μs.

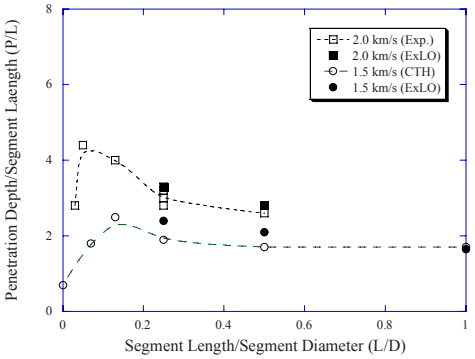

Fig. 7. Comparison of P/L versus L/D.

increases with increasing L/D. To evaluate the penetration efficiency, it is necessary to estimate the value of P/L, which is calculated for different aspect ratios at two impact velocities of 1.5 km/s and 2.0 km/s. The simulation results obtained from ExLO are shown in Fig. 7. Some experimental data [12] and CTH [15] simulation results are also compared in the figure. In general, the different methods show that the P/L increases with decreasing L/D. The ExLO prediction matches well with both the experimental data and CTH predictions.

4. Modeling of explosion

Blast waves in air and underwater explosion and the consequent damage to nearby structures have been of great interest in both defense science and protective system design industrial applications. Due to the extreme loading conditions, a state-of-the-art computational approach can be attractive. In this section the aim is to provide the Eulerian modeling of ExLO for the explosion events in air, in which generation and subsequent propagation of blast waves are simulated. The results are compared with an analytical solution. Air-shock is first simulated by using a one-dimensional spherical coordinate. A three-dimensional calculation is also conducted in rectangular coordinates to demonstrate the modeling capability in complex real problems.

4.1 Equation of state (EOS) for air blast

Development of the detonation product gases of the TNT is modeled with the standard Jones-Wilkins-Lee (JWL) equation of state (EOS). The equation [17] for pressure is,

$$P = A\left(1-\frac{\varpi}{R_1 V}\right)e^{-R_1 V} + B\left(1-\frac{\varpi}{R_2 V}\right)e^{-R_2 V} + \frac{\varpi E}{V} \quad (2)$$

where V is the volume of the material at pressure P divided by the initial volume of the unreacted explosive (non-dimensional value), and A, B, R_1, R_2, and ϖ are adjustable constants. Caution is required in the code implementation of the explosive initial energy since E is the internal energy per unit volume (=0.07 Mbar). Table 2 contains the unreacted equation of state parameters. It can also be noted that at large expansion ratio ($V \to \infty$), the first and second terms on the right hand side of Eq. (2) become negligible and hence the explosive can be assumed as an ideal gas. The density of TNT is 1630 kg/m^3. The values used for JWL TNT are obtained from the handbook [18].

Table 2. Equation of state parameters for unreacted TNT.

ρ_o (kg/m^3)	ϖ	A (Mbar)	B (Mbar)	R_1	R_2
1630	0.3	3.712	0.03231	4.15	0.95

Air is modeled as an ideal gas which uses a gamma law equation of state,

$$P = (\gamma - 1)\frac{\rho E}{\rho_o}, \quad (3)$$

where γ (=1.4) is the ratio of specific heats. The initial density of air, ρ_o, is 1.29 kg/m^3. The initial specific internal energy, E, is 0.1938 MPa in order to satisfy standard atmosphere pressure (0.1 MPa). Note that the unit of E is the unit of pressure.

4.2 One-dimensional spherical coordinate modeling

In this section, an one-dimensional spherically infinite computational domain has been considered. Numerical results are compared with an analytical equation for blast waves formed in air. The one-dimensional free-field model setup with a three-dimensional code is illustrated in Fig. 8. Non-rectangular hexahedron elements, whose top and bottom are parallel but whose sides have a slope of 0.01, were used to model the TNT and air medium. The dimensions used in this study are summarized in Table 3. The unit is (*m*, *sec*, *kg*), so the pressure is Pascal. To study computational grid sensitivity, the total number of cells of 500, 1000 and 2000 is included to a radius of 100 *m*. Since the uniform cell size is used throughout to the outer boundary, the initial size of the 9,080 kg explosive is modeled by 5 cells over its radius for I = 500 case. The same amount of TNT is modeled by 10 cells and 20 cells for I = 1,000 and I = 2000 cases, respectively.

The pressure signatures calculated at two locations (A, B) are displayed in Fig. 9, showing the typical blast waveforms. At shock arrival time, t_a, the pressure rises quickly to a peak pressure, $P_{\max}$, and returns to the ambient pressure. Then the pressure drops

Table 3. Computational dimensions in one-dimensional spherical coordinate.

$r_{i}(m)$	$r_{c}(m)$	$r_{t}(m)$	A (m)	B (m)
0.1	1.1	100.1	20.7	31.3

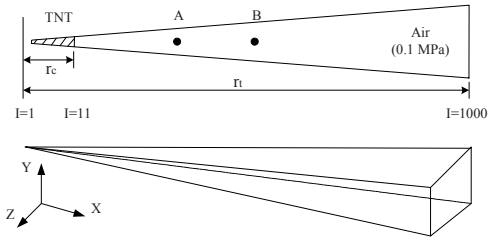

Fig. 8. One dimensional model setup (spherical coordinate) using a three-dimensional code.

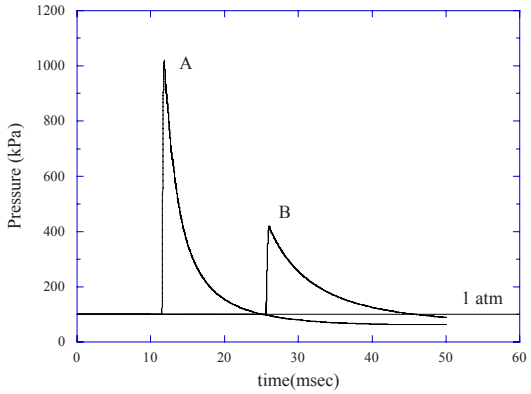

Fig. 9. Pressure signatures calculated at two different locations.

to a partial vacuum state causing a secondary shock at the later stage. Analytic equations to predict characteristics of blast waves in air have been provided in the referene [19]. For computer calculations, it is convenient to have the overpressure-distance data in analytic form and given by,

$$\frac{P^o}{P_a} = \frac{808\left[1+\left(Z/4.5\right)^2\right]}{\sqrt{1+\left(Z/0.048\right)^2}\sqrt{1+\left(Z/0.32\right)^2}\sqrt{1+\left(Z/1.35\right)^2}}, \quad (4)$$

where $P^o = P_{\max} - P_a$ and scaled distance Z ($m/kg^{1/3}$) is the distance away from explosive with an energy release of one kilogram TNT in the standard atmosphere. Since the shock velocity is uniquely related to

Table 4. Overpressure and shock arrival time comparisons from spherical coordinates.

	Scaled distance	Analytical	Numerical (mesh sensitivity)		
		Eqs. (4), (5)	I = 2000	I = 1000	I = 500
$(P_{\max}-P_a)/P_a$	A ($Z = 1.0$ $m/kg^{1/3}$)	10.15	9.17	8.72	7.74
	B ($Z = 1.5$ $m/kg^{1/3}$)	4.00	3.19	3.17	2.92
t_a (msec)	A	10.31	11.70	11.90	12.10
	B	22.65	25.82	25.95	26.40

overpressure ratio, the time required for that shock to travel out to various distances can be also given by,

$$t_a = \frac{1}{C_o}\int_{x_x}^{x}\left[\frac{1}{1+6P^o/7P_a}\right]^{0.5} dx, \quad (5)$$

where C_o is the speed of sound in the undisturbed atmosphere and x_c is the charge radius.

Table 4 summarizes the results for the peak pressure and shock arrival time from the numerical calculations and from the analytic Eqs. (4) and (5). A good agreement is obtained. The magnitudes of peak overpressure from predictions are somewhat underestimated compared to the analytic results, and this is also responsible for the delay of shock arrival time. It is academic to address that the analytic solution assumes a perfect discontinuity at the shock front, while a stiff enough shock front is inevitable in the numerical method due to the use of the artificial viscosity. Hence, the shock is allowed to spread to several cells resulting in a reduced peak and subsequently delayed shock front. Note that in the numerical solution the shock arrival time is estimated by the average between the time of first wave arrival and the time of peak wave arrival. The mesh sensitivity study indicates a resolved solution with a finer mesh of total number of cells of 2000.

Fig. 10 displays the pressure contours at several time steps to illustrate the shock wave propagation. As it propagates, the peak decays and the waveforms become broad. One interesting aspect from the contour is that a second wave is generated and starts to propagate at late stage shown in Fig. 10(c). At a late stage the explosive gas product becomes a partial

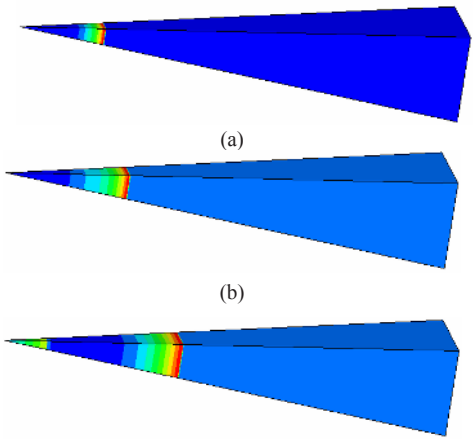

Fig. 10. Typical pressure contours from air shock, (a) 10 msec, (b) 20 msec, and (c) 40 msec.

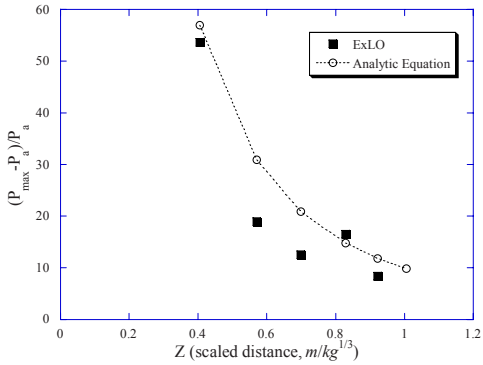

Fig. 11. Peak pressure decay along the propagation distance, three-dimensional calculation compared with air-blast analytical solution.

vacuum state due to over expansion caused by inertia. The ambient pressure is now relatively larger than the pressure inside the gas product and then a collapse phase starts. This contraction phase continues until the gas pressure becomes much larger than the surrounding fluid pressure and then a second expansion follows.

4.3 Three-dimensional rectangular coordinate modeling

For the purpose of addressing the possibility of a three-dimensional computational study, an extension of the previous one-dimensional model to a quarter of a block is considered in this section. The computational domain is a box and TNT is placed on a corner of the box. A first simulation was conducted with the total number of cells at 27,000 (30 x 30 x 30). A second simulation was with 216,000 (60 x 60 x 60). Equal length cells are used in this model. Again, development of the detonation product gases of the TNT is modeled with the standard JWL EOS, and the ideal gas EOS is used for air.

Fig. 11 shows the results for the peak pressure from the numerical calculations and from the analytic Eqs. (5) and (6). The scaled distance Z chosen for this three-dimensional study ranges from 0.5 to 1.0. Note that in the three-dimensional calculation the pressure sensors can be located arbitrarily at different angles with same distance from the charge. In general, the magnitudes of peak overpressure are underestimated compared to the analytic results. This trend is already

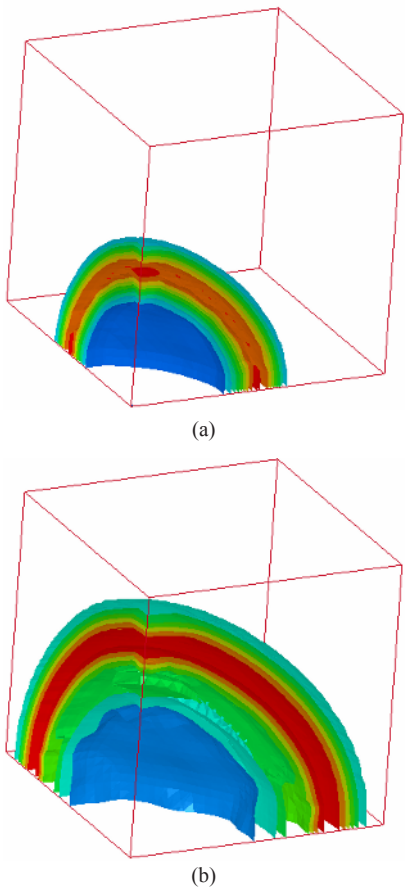

Fig. 12. Typical pressure contours in three-dimensional rectangular coordinates.

shown in the previous one-dimensional result. The problem presented here shows that ExLO can accurately predict explosion events. For the application of

ExLO to real complex design problems, it will be necessary to develop an efficient mesh generation technique in the future. Fig. 12 displays the pressure contours at two time steps. The spherical shock waves are well illustrated, and as the waves propagate the magnitude of the peak shock front decreases.

5. Conclusion

A new three-dimensional total shock physics code, ExLO, has been tested for highly transient problems involving large deformations associated with high-speed impact/penetration and explosion events. For both cases, Eulerian modeling is efficient or the only method to handle the mesh distortion problem naturally. Two high-speed impact problems are a long rod impact into a thick target and a disk-shaped segment impact into a thick target. ExLO predictions are compared well with previous experimental data. Other extreme loading conditions are the explosions. Here air-shocks are simulated in both a one-dimensional spherical coordinate system and three-dimensional rectangular coordinate system. The one-dimensional numerical results compared well with the air-blast analytical solution due to the resolved mesh resolution. However, the magnitude of peak shock pressure obtained from three-dimensional calculations is somewhat smaller than for the analytical solutions. This is the general feature occurring in the three-dimensional simulations. With more advances in both adaptive meshing and parallelization, ExLO may become an excellent analysis tool for design of extreme loading conditions.

Acknowledgment

Authors gratefully acknowledge the support by the Defense Acquisition Program Administration and Agency for Defense Development (UD070008AD).

References

[1] M. Lee and W. J. Chung, ExLO: A Three-Dimensional Total Shock Physics FEM Code, *J. of Mechanical Science and Technology*. 23 (2009) 1342-1353.

[2] D. J. Benson, Computational Methods in Lagrangian and Eulerian Hydrocodes, *Comput. Methods Appl. Mech. Engrg*., 99 (1992) 235-395.

[3] D. J. Benson and S. Okazawa, Contact in Multi-Material Eulerian Finite Element Formulation, *Comput. Methods Appl. Mech. Engrg*., 193 (2004) 4277-4298.

[4] L. I. Weingarten, M. F. Horstemeyser and W. P. Trento, Modeling Underwater Explosions with an Eulerian Code, *Proc. of the 63rd Shock and Vibration Symp.,* 269-277, (1992).

[5] P. Anninos, New VOF Interface Capturing and Reconstruction Algorithm, Lawrence Livermore National Lab., UCRL-ID-135084 (1999).

[6] D. L. Youngs, An Interface Tracking Method for a 3D Eulerian Hydrodynamics Code, Tech. Report AWRE/44/92/35, AWRE Design Mathematics Division, UK (1987).

[7] D. L. Young, Time Dependent Multi-Material Flow with Large Fluid Distortion, *Numerical Methods for Fluid Dynamics*, edited by K.W. Morton and M.J. Baines, Academic Press (1982).

[8] B. van Leer, Towards the Ultimate Conservative Difference Scheme, IV. A New Approach to Numerical Convection, *J. Comp. Phys*., 23 (1977) 276-299.

[9] D. J. Benson, Momentum Advection on a Staggered Mesh, *J. Comp. Phys*., 100 (1992) 143-162.

[10] C. E. Anderson, J. D. Walker, S. J. Bless and Y. Partom, On the L/D Effect for Long-Rod Penetrators, *Int. J. Impact Engng*., 18 (1996) 247-264.

[11] J. A. Zukas, Numerical Simulation of Semi-Infinite Target Penetration by Continuous and Segmented Rods, Report No. BRL-TR-3081, Army Ballistic Research Lab, Aberdeen Proving Ground, MD (1990).

[12] T. W. Bjerke, J. A. Zukas and K. D. Kimsey, Penetration Performance of Disk Shaped Penetrators, *Int. J. Impact Engng*., 12 (2) (1992) 263-280.

[13] D. L. Orphal, C. E. Anderson, R. R. Franzen, J. D. Walker, P. N. Schneidewind and M. E. Majerus, Impact and Penetration by L/D < 1 Projectiles, *Int. J. Impact Engng*., 14 (1993) 551-560.

[14] R. R. Franzen, J. D. Walker, D. L. Orphal and C. E. Anderson, An Upper Limit for the Penetration Performance of Segmented Rods with Segment-L/D<1, *Int. J. Impact Engng*., 15 (5) (1994), 661-668.

[15] J. D. Walker, A Model for Penetration by Very Low Aspect Ratio Projectiles, *Int. J. Impact Engng*., 23 (1999), 957~966.

[16] M. Lee and M. J. Normandia, Successive Impact of Segmented Rods at High-Velocity, *KSME Int. Journal,* 13 (4) (1999), 312-320.

[17] E. L. Lee and C. M. Tarver, Phenomenological

Model of Shock Initiation in Heterogeneous Explosives, *Physics of Fluids*, 23 (12) (1980), 2362~2372.
[18] B. M. Dobratz, LLNL Explosive Handbook, UCRL-52997, Lawrence Livermore National Laboratory, Livermore, CA. USA (1981).
[19] G. F. Kinney and K. J. Graham, Explosive Shocks in Air, 2nd Edition, Springer-Verlag (1985).

Minhyung Lee. Professor in the Mechanical and Aerospace Engineering at the Sejong University, Seoul, Korea, holds a PhD from the University of Texas at Austin. His research interests include Lagrangian, Multi-material Eulerian and arbitrary Lagrangian-Eulerian (ALE) finite element methods for high strain rate of large deformation problems (eg, high speed impact/penetration, air blast/underwater explosion and bubble dynamics). Prior to joining Sejong University, he was with the US Naval Postgraduate School, Monterey, CA. as a research professor working on the UNDEX problems. He was also with the Institute for Advanced Technology, Austin, TX. (federated with Army Research Lab.) working on the highly transient dynamics.

Wanjin Chung. Professor in the Die and Mould Engineering at the Seoul National University of Technology, Seoul, Korea, holds a PhD from Korea Advanced Institute of Technology. His research interests include the development of finite element methods for large deformation problems and its application to metal forming problems (eg, sheet metal forming, forging, high-velocity forming). Prior to joining Seoul National University of Technology, he works at Samsung Advanced Institute of Technology, Kiheung, Korea, as a senior researcher.